Inorganic Chemistry

ARTICLE

pubs.acs.org/IC

Characterization and Properties of Novel Gallium-Doped Calcium Phosphate Ceramics

Charlotte Mellier,[†,⊥,∥] Franck Fayon,[*,‡,§] Verena Schnitzler,[†] Philippe Deniard,[#] Mathieu Allix,[‡,§] Sophie Quillard,[⊥] Dominique Massiot,[‡,§] Jean-Michel Bouler,[⊥] Bruno Bujoli,[*,∥] and Pascal Janvier[∥]

[†]Graftys SA, Eiffel Park, Bâtiment D, 415 Rue Claude Nicolas Ledoux, Pôle d'activités d'Aix en Provence, 13854 Aix en Provence CEDEX 3, France

[‡]CNRS, UPR 3079, CEMHTI, 1D Avenue de la Recherche Scientifique, 45071 Orléans Cedex 02, France

[§]Université d'Orléans, Faculté des Sciences, Avenue du Parc Floral, BP 6749, 45067 Orléans Cedex 2, France

[⊥]Université de Nantes, INSERM, UMR 791, LIOAD, Faculté de Chirurgie Dentaire, BP 84215, 44042 Nantes Cedex 1, France

[∥]Université de Nantes, CNRS, UMR 6230, CEISAM, 2 Rue de la Houssinière, BP 92208, 44322 NANTES Cedex 3, France

[#]Institut des Matériaux Jean Rouxel, Université de Nantes, UMR CNRS 6502, 2 Rue de la Houssinière, BP 32229, 44322 Nantes Cedex 3, France

Supporting Information

ABSTRACT: Addition of a gallium (Ga) precursor in the typical reaction protocols used for the preparation of β-tricalcium phosphate (β-TCP) led to novel Ga-doped β-TCP ceramics with rhombohedral structures (*R*3*c* space group). From the refinement of their X-ray diffraction patterns, it was found that the incorporation of Ga in the β-TCP network occurs by substitution of one of the five calcium (Ca) sites, while occupation of another Ca site decreases in inverse proportion to the Ga content in the structure. The Ga local environment and the modification of the phosphorus environments due to the Ga/Ca substitution in Ga-doped β-TCP compounds are probed using ^{31}P and ^{71}Ga magic-angle spinning NMR. A decrease of the unit cell volume is observed with increasing Ga content, together with improved mechanical properties. Indeed, the compressive strength of these new bioceramics is enhanced in direct proportion of the Ga content, up to a 2.6-fold increase as compared to pure β-TCP.

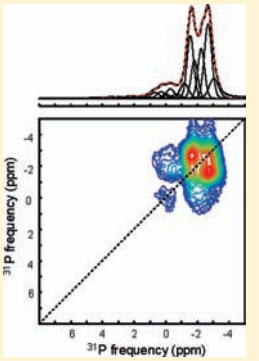

1. INTRODUCTION

Porous calcium phosphate ceramics (CaPs) have been used extensively as bioactive implants in human bone surgery, due to their similarity to the mineral component of bone.[1−9] Indeed, such biomaterials with suitable composition and porosity are slowly resorbed in the body, to be replaced by natural bone by the same processes active in bone remodeling. If combined with drugs, then bone substitute materials when implanted might in addition be also well-suited to address bone-related diseases, such as osteoporosis.[10−24] Current approaches for the prevention and the treatment of osteoporosis consist in systemic therapies, the purpose of which is most often increasing bone density by decreasing osteoclastic bone resorption using drugs, among which bisphosphonates are the most commonly used, as compared, for example, to selective estrogen receptor modulators (SERM), strontium ranelate, and various types of hormones. However, the effect on bone healing is limited in some cases due to poor bioavailability of the drug, which cannot be administered at higher doses because of significant side effects. Finally, in the case of bisphosphonate medication, low therapeutic compliance is one important problem for osteoporotic patients.[25]

Many studies have shown that gallium (Ga) inhibits bone resorption and, when present, lowers concomitant elevated plasma calcium,[26−28] leading to its use in the clinical treatment of hypercalcemia of malignancy and Paget's disease of bone.[29,30] Accordingly, it has been suggested as a treatment for osteoporosis. Gallium nitrate is currently marketed by Genta as the FDA approved labeling Ganite. This product is administered through intravenous injection for the treatment of clearly symptomatic cancer-related hypercalcemia that has not responded to adequate hydration. While gallium nitrate acts as a potent inhibitor of bone density breakdown, this drug presents two major drawbacks: (i) a very low bioavailability and (ii) the need for a long and continuous intravenous administration, resulting in a potential toxicity. The design of an implantable gallium-doped scaffold usable for the release of gallium in vivo would potentially offer a better

Received: April 15, 2011
Published: July 27, 2011

bioavailability of Ga(III) ions, in osteoporotic sites. Indeed, using osteoclastic and osteoblastic cell lines we have recently demonstrated that Ga^{3+} ions in solution exhibited a dose-dependent (0−100 μM) antiosteoclastic effect, by reducing in vitro osteoclastic resorption, differentiation, and formation without negatively affecting osteoblastic bone forming cells.[31] Accordingly, these results suggested that gallium may be a promising candidate for the development of a bone bioactive drug delivery system (DDS) targeting osteoporotic sites.

Since gallium has long been known to concentrate in skeletal tissue, particularly regions of bone deposition and remodeling[32,33] and to adsorb in vitro to synthetic hydroxyapatite,[34,35] we have investigated the design of gallium-doped phosphocalcic compound usable for the release of gallium in vivo. To date, very few studies have reported the preparation of gallium-doped calcium phosphates, mainly based on hydroxyapatite[36] or brushite.[37] In this context, the β-tricalcium phosphate (β-TCP) structure seemed to be a good candidate for gallium-doping, since the incorporation of different cations by substitution of some calcium sites in the β-TCP network was reported in the literature (Na^+, Zn^{2+}, Mg^{2+}, Sr^{2+}, Cu^{2+}, Co^{2+}),[38−45] including trivalent ions (In^{3+}, Fe^{3+}),[46,47] leading to compounds of formula $Ca_{10.5-zx/2}M^z_x(PO_4)_7$, where M is a cation and z its oxidation state. In addition, β-TCP ceramics are widely used as bone substitutes, and their good in vivo solubility should favor the in situ release of the gallium ions.

Therefore, the preparation of gallium-doped β-TCP phases was investigated in the present study according to different methods, including direct solid-phase synthesis along with calcination of gallium-loaded calcium-deficient apatite precursors obtained by soft chemistry routes. In this article, we demonstrate on the basis of electron diffraction and X-ray powder diffraction (XRD) analyses that the resulting gallium-doped β-TCP compounds adopt a rhombohedral structure with $R3c$ space group, in which only one of the calcium sites can be partly replaced by gallium, leading to a nonlinear contraction of the unit cell volume. The modification of the phosphorus local environments due to the Ca/Ga substitution are characterized using ^{31}P and $^{31}P-^{71}Ga$ double resonance solid-state NMR.

2. EXPERIMENTAL SECTION

Synthesis. *Preparation of $Ca_{10.5-1.5x}Ga_x(PO_4)_7$ by Solid-State Reaction.* In a mortar, anhydrous calcium phosphate (0.174 mol) was intimately mixed with the quantity of calcium carbonate, and gallium oxide calculated so that the (Ca + Ga)/P molar ratio corresponds to the desired x value according to eq 1.

$$7CaHPO_4 + (3.5 - 1.5x)CaCO_3 + x/_2Ga_2O_3 \rightarrow Ca_{10.5-1.5x}Ga_x(PO_4)_7 + 3.5H_2O + (3.5 - 1.5x)CO_2 \quad (1)$$

The mixture was ground for 30 min and sintered at 1000 °C for 24 h, typically on a 5 g preparation scale (heating rate: 5 °C/min, cooling rate: 5 °C/min).

Preparation of $Ca_{10.5-1.5x}Ga_x(PO_4)_7$ Using a Two-Step Coprecipitation/Calcination Process. In a typical procedure, a mixture of gallium nitrate hydrate and calcium nitrate tetrahydrate was dissolved in a beaker containing 125 mL of ultrapure water, with a (Ca + Ga)/P molar ratio of 1.515 and a Ga/Ca molar ratio in the 0−0.08 range. The pH of the solution was adjusted in the 9−9.5 range by means of a concentrated solution of ammonia. The reaction mixture was then introduced in a three-neck angled round-bottom flask placed in an oil bath and equipped with a dropping funnel. The temperature of the reaction mixture was raised to 50 °C, and 1.089 g of diammonium hydrogen phosphate (8.25 mmol) dissolved in 125 mL of ultrapure water was added dropwise over a 5−10 min period. The mixture turned white, and the pH was adjusted in the 7.5−8 range by means of a concentrated solution of ammonia. After 30 min, the mixture was allowed to cool, and the suspension (pH was neutral) was filtered off and washed with 250 mL of ultrapure water. After repeating this procedure four times, the white waxy product was dried in an oven at 80 °C for 24 h. The gallium content of the collected aqueous fractions was measured by atomic absorption spectroscopy to determine the amount of gallium incorporated in the isolated solid phase.

After calcination at 1000 °C for 4 h, the resulting compounds led to $Ca_{10.5-1.5x}Ga_x(PO_4)_7$ compounds, where x varied in the 0−0.75 range, as a function of the initial Ca/Ga molar ratio.

Materials and Methods. *X-ray Powder Diffraction.* The XRD patterns of β-$Ca_{10.5-1.5x}Ga_x(PO_4)_7$ powders were recorded using a Bruker D8 Advance diffractometer (Bragg−Brentano, $\theta/2\theta$ geometry) equipped with a copper anode, a germanium monochromator ($CuK_{\alpha 1}$) and a Vantec position-sensitive detector for fast data collection despite the large unit cell of the compound (6−110° 2θ range with a 0.017° 2θ step at 3.5s/step). Rietveld refinements were carried out to determine the unit cell parameters and the atomic positions using JANA 2006[48] code for Rietveld refinement with the fundamental parameters approach[49] to directly take into account the instrumental contribution to Bragg peaks profile during the refinement procedure. The location of gallium was based on the M5 site occupation fraction, making the initial hypothesis that this site was fully occupied by calcium. The obtained value being higher than 100% was the indication of a substitution of this site by a heavier atom. This substitution has been then introduced subsequently into the refinement. TiO_2 anatase powder (Merck) (around 10% w/w) was mixed with the samples for accurate amorphous phase percentage determination.[50]

Solid-State NMR. All ^{31}P solid-state magic angle spinning (MAS) NMR experiments were performed on a Bruker Avance 300 spectrometer operating at 7.0 T (^{31}P Larmor frequency of 121.5 MHz) using a 4 mm double-resonance MAS probe. The quantitative ^{31}P one-dimensional (1D) single pulse MAS spectra were acquired using a small pulse length (0.8 μs, 20° flip angle) and a long recycle delay of 60 s to ensure no saturation. The ^{31}P two-dimensional (2D) through-space double quantum−single quantum (DQ-SQ) MAS correlation spectra were recorded at a spinning frequency of 10 kHz. The POST7 DQ recoupling sequence[51] with a ^{31}P nutation frequency of 70 kHz was used for the excitation and reconversion of DQ coherences. The DQ excitation and reconversion times were fixed to 1.4 ms, corresponding to 14 rotor periods. To reduce the overall acquisition times of the 2D experiments, recycle delays of 20s with presaturation loops were employed. Pure absorption phase spectra were obtained using the States method,[52] and 90 rotor-synchronized t_1 increments of 400 μs (i.e., four rotor periods) with 16 scans each were collected.

^{71}Ga and $^{71}Ga-^{31}P$ double resonance solid-state NMR experiments were performed on a Bruker Avance 750 spectrometer operating at 17.6 T (^{71}Ga and ^{31}P Larmor frequencies of 228.77 and 303.66 MHz, respectively) using a 4 mm triple-resonance MAS probe. The ^{71}Ga 1D MAS central transition spectra were recorded at a spinning frequency of 14 kHz using a Hahn echo sequence with a ^{71}Ga nutation frequency of 9 kHz (central transition selective 90° pulse length of 13.9 μs) and a recycle delay of 1s. The spinning frequency was 14 kHz, and the τ delay was set to one rotor period. ^{31}P {^{71}Ga}-edited 1D and $^{71}Ga-^{31}P$ 2D HETCOR MAS spectra were recorded at a spinning frequency of 14 kHz using the R^3-heteronuclear multiple quantum coherence (HMQC) experiment.[53,54] The ^{31}P and ^{71}Ga 90° pulse lengths were 7.5 and 14 μs, respectively. Recoupling of the $^{31}P-^{71}Ga$ heteronuclear dipolar interaction under MAS was achieved using a continuous wave ^{31}P pulse spanning on 15 rotor periods with a radio frequency (RF) field

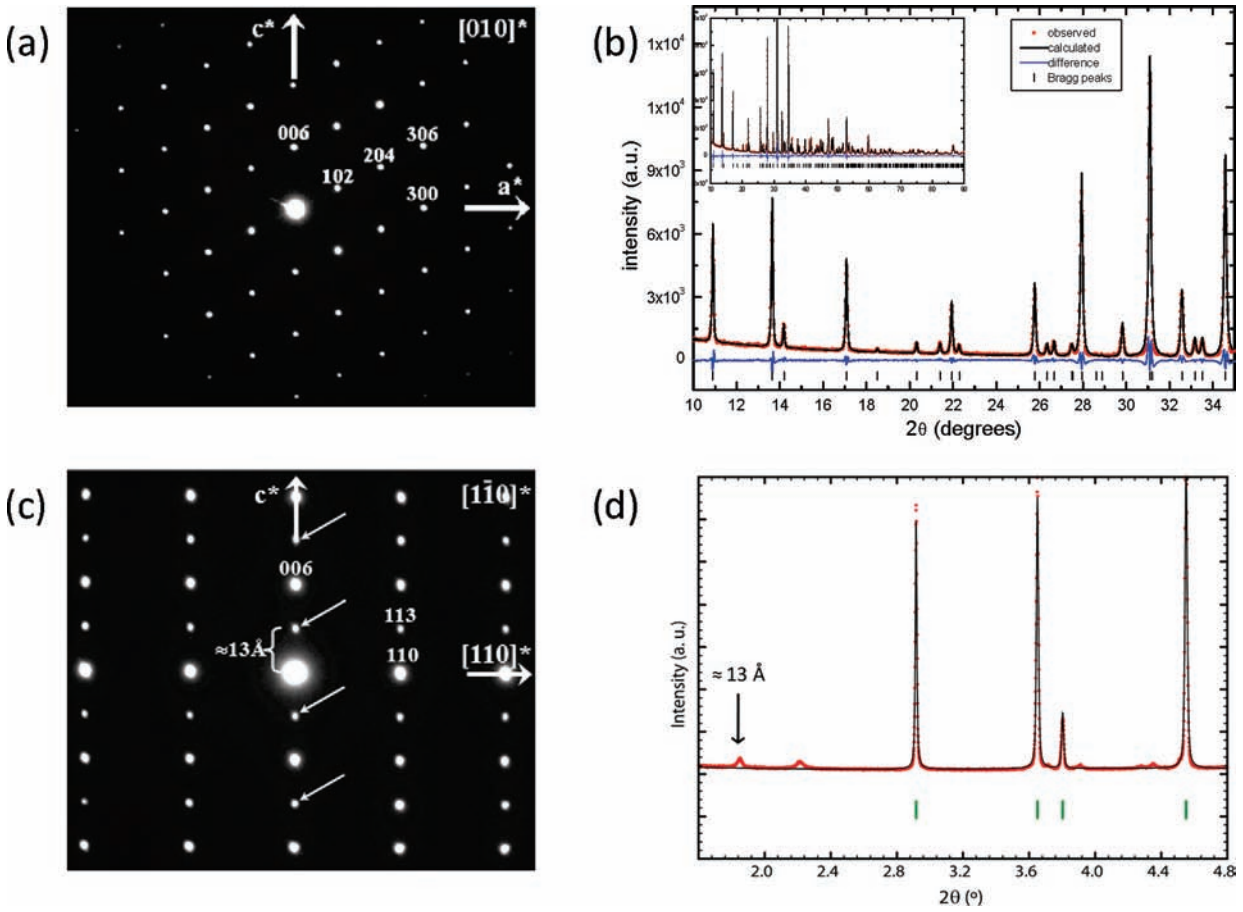

Figure 1. (a) Experimental [010] electron diffraction pattern and (b) experimental and calculated powder XRD patterns of $Ca_{10.5-1.5x}Ga_x(PO_4)_7$ for $x = 0.45$ (x value obtained from the Rietveld structural refinement of the XRD pattern of a sample synthesized from solid-state reaction). In (b), the Bragg positions (vertical ticks) and the differences between experimental and calculated data (in blue) are shown. The fit statistics are $R_p = 9.56\%$, $R_{wp} = 13.15\%$, and $R_{Bragg} = 3.31\%$. (c) The experimental [1−10] electron diffraction pattern of $Ca_{10.5}(PO_4)_7$ (pure β-TCP) is given for comparison. In (c), the arrows indicate additional diffraction spots not allowed by the $R3c$ symmetry, which can either be due to double reflection or to a lower symmetry superstructure. (d) Synchrotron powder diffraction pattern ($\lambda = 0.41397$ Å, 11BM diffractometer, APS, Argonne National Laboratoty) of pure β-TCP evidencing weak-intensity reflections not allowed by $R3c$ symmetry. These additional reflections could not be assigned to any other known calcium phosphate phase and perfectly correspond to the extra spots observed by electron diffraction (see arrows), therefore suggesting a lower symmetry superstructure.

strength of 14 kHz (i.e., satisfying the $n = 1$ rotary resonance condition). Pure absorption phase 2D HETCOR spectra were obtained using the States method,[52] and 52 rotor-synchronized t_1 increments of 143 μs (i.e., two rotor periods) with 3840 scans each were collected.

^{31}P and ^{71}Ga chemical shifts were referenced relative to a 85% H_3PO_4 solution and a 1.1 mol·kg^{-1} $Ga(NO_3)_3$ D_2O solution, respectively. Simulations of all spectra were performed using the dmfit software.[55]

3. RESULTS AND DISCUSSION

3.1. Structural Characterization of Gallium-Doped β-TCP Ceramics Using Electron Diffraction, Powder XRD, and Multinuclear Solid-State NMR Spectroscopy. Our attempts to prepare gallium-doped β-TCP ceramics were derived from two methods commonly reported in the literature for the synthesis of pure β-TCP:

(i) sintering of a $CaHPO_4/CaCO_3$ mixture, to which Ga_2O_3 was added using the suitable stoichiometry from eq 1.

(ii) calcination of calcium-deficient apatites (CDAs) synthesized by precipitation in the presence of gallium nitrate with a (Ca + Ga)/P molar ratio of 1.515. For the preparation of the CDA precursors, the selected base was ammonium hydroxide. Indeed, we have previously reported that CDAs prepared in the presence of sodium resulted after calcination in the incorporation of sodium in the β-TCP network, by substitution of some calcium sites.[39]

The structure of pure β-TCP was determined by single-crystal XRD by Dickens et al.[56] and later confirmed by Yashima et al.[57] through a neutron powder diffraction study. For both preparation routes used in the present work, both the electron diffraction and the powder XRD patterns of the obtained ceramics show that the average structure of Ga-doped β-TCP is rhombohedral with the $R3c$ symmetry, similar to the β-TCP proposed structure.[56,57] For all the studied Ga-doped ceramics, the electron diffraction patterns show very well-defined dots indicative of highly crystalline samples and no extra spots (or diffuse streaks) than those expected for the $R3c$ structural model. Typical electron diffraction and powder XRD patterns obtained for the $Ca_{10.5-1.5x}Ga_x(PO_4)_7$ samples are shown in Figure 1a and b. Energy-dispersive X-ray spectrometry (EDXS) analyses indicated

dx.doi.org/10.1021/ic2007777 |Inorg. Chem. 2011, 50, 8252–8260

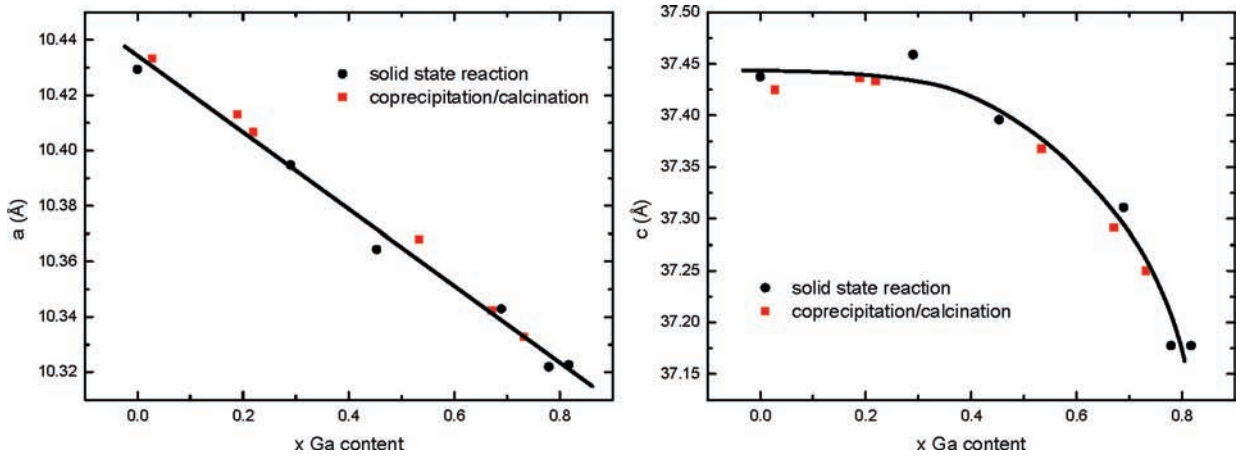

Figure 2. Variation of the cell parameters obtained from Rietveld structural refinements of $Ca_{10.5-1.5x}Ga_x(PO_4)_7$ compounds prepared by both solid-phase and coprecipitation/calcination reactions, as a function of the x Ga content obtained from the refinement. The a and c values for pure β-TCP [a = 10.4352(2) Å, c = 37.4029(5) Å] are given for comparison.[57]

Table 1. Positional and Thermal Parameters for the Atoms of $Ca_{10.5-1.5x}Ga_x(PO_4)_7$ for x = 0.45[a]

atom	site	symmetry	occupancy	x	y	z	U_{iso} (Å^2)
Ca1	18b	1	1	0.7255(6)	0.8580(10)	0.1674(3)	0.0097(9)
Ca2	18b	1	1	0.6228(6)	0.8250(11)	−0.0328(3)	0.0097
Ca3	18b	1	1	0.1282(8)	0.2766(5)	0.0608(3)	0.0097
M5/Ga1	6a	3.	0.441(14)	0	0	−0.264	0.008(2)
M5/Ca5	6a	3.	0.559(14)				
M4/Ca4	6a	3.	0.280(7)	0	0	−0.0615(10)	0.0097
P1	6a	3.	1	0	0	−0.0001(4)	0.009(2)
P2	18b	1	1	0.6806(8)	0.8573(12)	−0.1289(3)	0.009
P3	18b	1	1	0.6500(11)	0.8457(12)	−0.2333(3)	0.009
O1	6a	3.	1	0	0	0.0499(8)	0.004(2)
O2	18b	1	1	0.0207(18)	0.8685(14)	−0.0087(6)	0.004
O3	18b	1	1	0.7347(18)	0.9130(18)	−0.0925(6)	0.004
O4	18b	1	1	0.770(2)	0.781(2)	−0.1445(6)	0.004
O5	18b	1	1	0.732(3)	0.008(3)	−0.1541(6)	0.004
O6	18b	1	1	0.5104(19)	0.760(3)	−0.1382(5)	0.004
O7	18b	1	1	0.608(2)	0.956(2)	−0.2193(7)	0.004
O8	18b	1	1	0.590(2)	0.694(2)	−0.2136(6)	0.004
O9	18b	1	1	0.819(2)	0.916(3)	−0.2297(5)	0.004
O10	18b	1	1	0.6285(16)	0.826(2)	0.7254(6)	0.004

[a] Cell parameters (Å, °): 10.36429(19), 10.36429, 37.3959(9), 90.0, 90.0 120.0.

relatively homogeneous gallium content within crystallites, at least at the probe scale (less than 50 nm). The presence of chemical composition inhomogeneity at a smaller length scale, which would give rise to extra features on electron diffraction patterns, was thus excluded.

Rietveld refinement of the XRD patterns of the various samples, mixed with TiO_2 to detect the presence of any amorphous impurity, showed a monotonic variation in cell parameters. A linear decrease of the a parameter and a monotonic decrease of the c parameter were observed (Figure 2), leading to a contraction of the cell volume as the gallium content increased. This behavior was expected considering the differences between both cationic radius and oxidation state of gallium compared to calcium (0.99 Å (Ca^{2+}) and 0.62 Å (Ga^{3+})).

The JANA 2006 program was successfully used to refine the structure for various Ga/Ca ratios, which corresponded to the $Ca_{10.5-1.5x}Ga_x(PO_4)_7$ general formula. Based on the proposed β-TCP crystal structure, gallium ions only occupy the M5 calcium site, while calcium occupation of the M4 site decreases in inverse proportion to the gallium content in the structure (Table 1). This substitution mechanism is similar to that previously described for trivalent cations in the case of In^{3+}- and Fe^{3+}-doped β-TCP.[46,47] The atomic parameters of the $Ca_{10.5-1.5x}Ga_x(PO_4)_7$ compound with x = 0.45 are gathered in Table 1. For all the studied samples, the Ga content was determined using constraints on atom site occupation factors to ensure the charge balance of the material.

Irrespective of the preparation method, for initial Ga/Ca molar ratio less than 0.075, the amount of gallium in the final

dx.doi.org/10.1021/ic2007777 |Inorg. Chem. 2011, 50, 8252–8260

Table 2. Ga wt% Content in The $Ca_{10.5-1.5x}Ga_x(PO_4)_7$ Final Products

		Ga wt% in the final product	
entry	Initial Ga/Ca ratio	AAS[a]	XRD[b]
1	0.025[c]	1.58 ± 0.25	1.86
2	0.052[d]	3.16 ± 0.25	3.32
3	0.074[c]	4.47 ± 0.25	4.40
4	0.092[d]	5.42 ± 0.25	4.65
5	0.11[c]	6.19 ± 0.25	5.23

[a] Determined by atomic absorption spectroscopy. [b] Determined from the Rietveld refinement of the experimental XRD patterns, assuming that a pure $Ca_{10.5-1.5x}Ga_x(PO_4)_7$ structure is obtained. [c] Determined by compound obtained by solid-phase reaction. [d] Determined by compound prepared via a coprecipitation/calcination route.

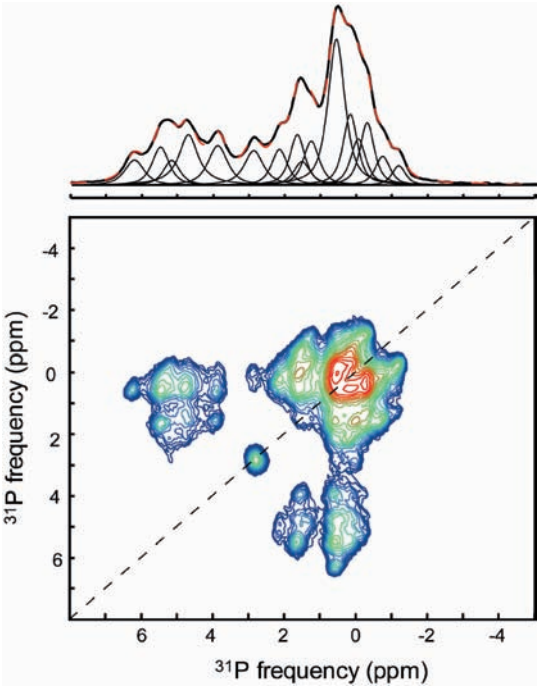

Figure 3. ^{31}P 2D sheared homonuclear DQ−SQ correlation MAS NMR spectrum of β-$Ca_{10.5}(PO_4)_7$ recorded at B_0 = 7.0 T using the POSTC7 DQ dipolar recoupling pulse sequence with a spinning frequency of 10 kHz. The experimental and reconstructed ^{31}P single pulse MAS NMR spectra of β-$Ca_{10.5}(PO_4)_7$ are shown above the 2D spectrum.

product measured by atomic absorption spectroscopy was found to be close to that expected for a quantitative incorporation of gallium in the β-TCP structure. Indeed, the Ga wt% determined by atomic absorption spectroscopy was fully consistent with that obtained from the XRD Rietveld refinements, considering the presence of a $Ca_{10.5-1.5x}Ga_x(PO_4)_7$ single phase (Table 2, entries 1−3). However, deviation between these two values was observed for higher initial Ga/Ca molar ratios (Table 2, entries 4−5), due to the presence of side products, the major part of which corresponding to an unidentified amorphous component (i.e., 15 wt % for a 0.11 Ga/Ca ratio) and to a lower extent to crystalline β-$Ca_2P_2O_7$ pyrophosphate (3.5 wt%).

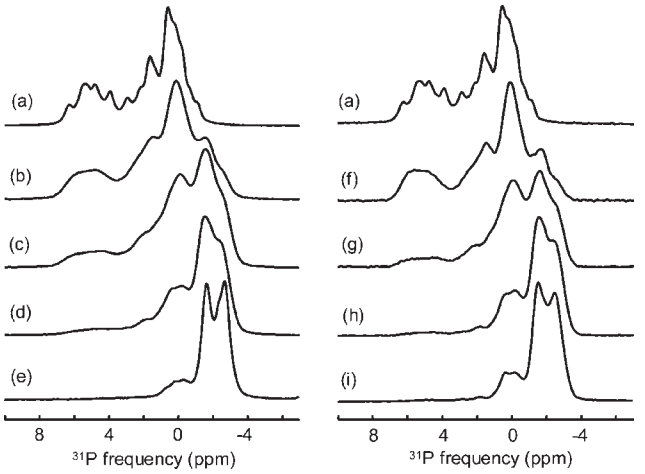

Figure 4. ^{31}P single pulse MAS NMR spectra of $Ca_{10.5-1.5x}Ga_x(PO_4)_7$ compounds with: (a) x = 0, (b) x = 0.29 (initial Ga/Ca = 0.025), (c) x = 0.45 (initial Ga/Ca = 0.046), (d) x = 0.69 (initial Ga/Ca = 0.074), (e) x = 0.82 (initial Ga/Ca = 0.11) [synthesized by solid-state reaction], (f) x = 0.22 (initial Ga/Ca = 0.021), (g) x = 0.52 (initial Ga/Ca = 0.052), (h) x = 0.67 (initial Ga/Ca = 0.070), and (i) x = 0.73 (initial Ga/Ca = 0.092) [synthesized using the coprecipitation/calcination process].

To investigate the structural modification of the phosphorus environments due to the Ca/Ga substitution in the β-TCP network, ^{31}P solid-state MAS NMR spectra of $Ca_{10.5-1.5x}Ga_x(PO_4)_7$ samples and pure β-TCP were also recorded. The proposed β-TCP structure involves three fully occupied crystallographically distinct phosphorus sites with Wyckoff multiplicities of 6 (P1) and 18 (P2, P3), while the calcium ions are distributed over five different sites. Two of these Ca sites [M4 and M5] are located in special positions, one of which is half occupied [M4].[56,57] As shown in Figure 3, the ^{31}P MAS NMR spectrum of pure β-TCP exhibits a large number of partly overlapping resonances. Enhanced spectral resolution of the various P sites was obtained using a 2D ^{31}P homonuclear DQ−SQ correlation experiment which allowed resolving overlapping ^{31}P resonances having similar isotropic chemical shifts but different P neighbors.[58] From the obtained 2D correlation spectrum, 16 distinct ^{31}P narrow resonances (^{31}P linewidths range from 0.45 to 0.65 ppm) can be distinguished, with significantly different relative intensities indicating that β-TCP contains at least 16 inequivalent P sites. Such narrow resonances would not be expected assuming a random distribution of the vacancies in the structure, since the resulting positional disorder around the phosphorus atoms should significantly broaden the ^{31}P resonances. This strongly suggests an ordering of the vacancies within the β-TCP structure.

Preliminary investigation of the vacancies ordering within the β-TCP structure has been carried out on the basis of ^{31}P isotropic chemical shifts PBE-DFT calculations[59] for several structural models using the GIPAW method[60] implemented in the CASTEP code.[61,62] For three basic possible arrangements of half occupying M4 site within the 1 × 1 × 1 β-TCP structure described by Jay et al.,[63] which exhibits space groups of lower symmetry ($P3$ and $R3$ for the lowest-energy configuration), the theoretically calculated ^{31}P MAS NMR spectra exhibit a much smaller number of ^{31}P resonances (i.e., of distinct P sites) than that observed in our experimental spectrum. This suggests that crystalline β-TCP likely adopt a superstructure. As shown in Figure 1c and d, electron and synchrotron powder diffraction

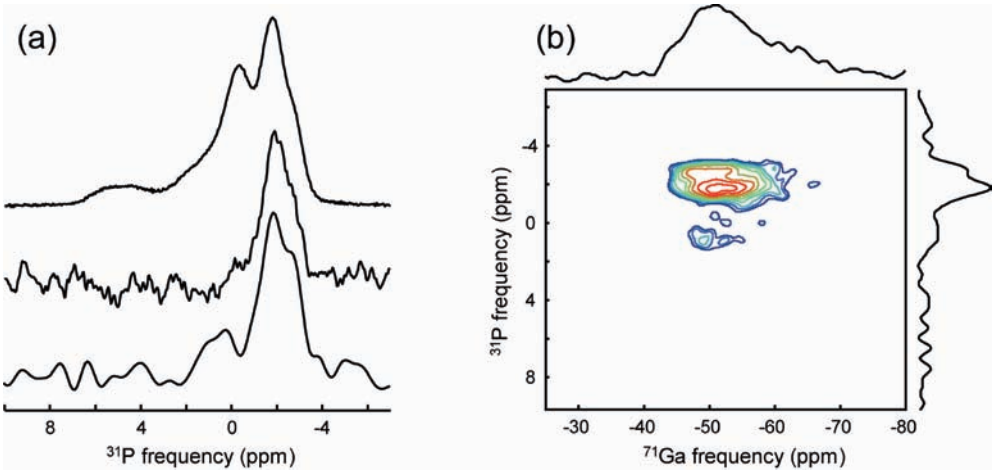

Figure 5. (a) 1D ^{31}P quantitative single pulse MAS spectrum (top), 1D ^{31}P $\{^{71}$Ga$\}$-edited MAS spectrum (middle) and projection along the ^{31}P dimension of the 2D ^{71}Ga−^{31}P HETCOR MAS spectrum shown in (b) (bottom) obtained for the $Ca_{10.5-1.5x}Ga_x(PO_4)_7$ sample with $x = 0.45$ (initial Ga/Ca = 0.046). All spectra were recorded at a magnetic field of 17.6 T with a spinning frequency of 14 kHz.

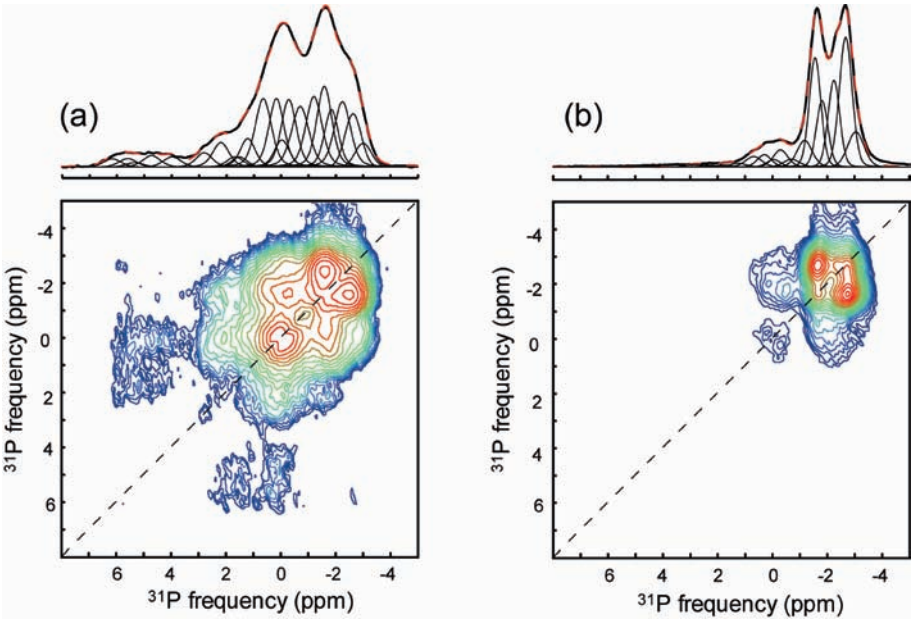

Figure 6. ^{31}P 2D sheared homonuclear DQ−SQ correlation MAS NMR spectra of $Ca_{10.5-1.5x}Ga_x(PO_4)_7$ compounds with (a) $x = 0.52$ (initial Ga/Ca = 0.052) and (b) $x = 0.82$ (initial Ga/Ca = 0.11). The 2D spectra were recorded at $B_0 = 7.0$ T using the POSTC7 DQ dipolar recoupling pulse sequence with a spinning frequency of 10 kHz. The corresponding experimental (black) and reconstructed (red dotted line) ^{31}P single pulse MAS NMR spectra are shown above the 2D spectra.

data provide further experimental evidence for the presence of a superstructure with symmetry lower than *R*3c.

As already discussed from diffraction results, gallium insertion in the structure appears to take place on the M5 site (surrounded by the P2 and P3 phosphorus sites) with concomitant decrease of the calcium occupancy in the M4 site. The ^{31}P isotropic chemical shift being very sensitive to local structural modifications, the introduction of gallium in the structure results in the appearance of additional ^{31}P resonances with isotropic chemical shifts in the −1.5/−3.0 ppm range, assigned to Ga-neighboring P2 and P3 sites (Figure 4). It should also be noted that the ^{31}P resonances in the spectra of the $Ca_{10.5-1.5x}Ga_x(PO_4)_7$ compounds are broadened even for very low Ga contents, by comparison with pure β-TCP. This broadening suggests a random Ca/Ga substitution that suppresses the long-range ordering of the vacancies in the β-TCP structure. This is consistent with the absence of extra spots on the electron diffraction patterns which give evidence that the average structure of $Ca_{10.5-1.5x}Ga_x(PO_4)_7$ compounds is correctly described by the proposed 1 × 1 × 1 cell *R*3*c* model.

The assignment of the additional ^{31}P resonances observed in Ga-doped β-TCP compounds to P sites having Ga neighbors is supported by 1D ^{31}P $\{^{71}$Ga$\}$-edited and 2D ^{71}Ga−^{31}P heteronuclear correlation (HETCOR) MAS spectra. As clearly shown in Figure 5, only the ^{31}P resonances in the −1.5/−3.0 ppm range are observed in these heteronuclear dipolar recoupling experiments.

dx.doi.org/10.1021/ic2007777 |*Inorg. Chem.* 2011, 50, 8252–8260

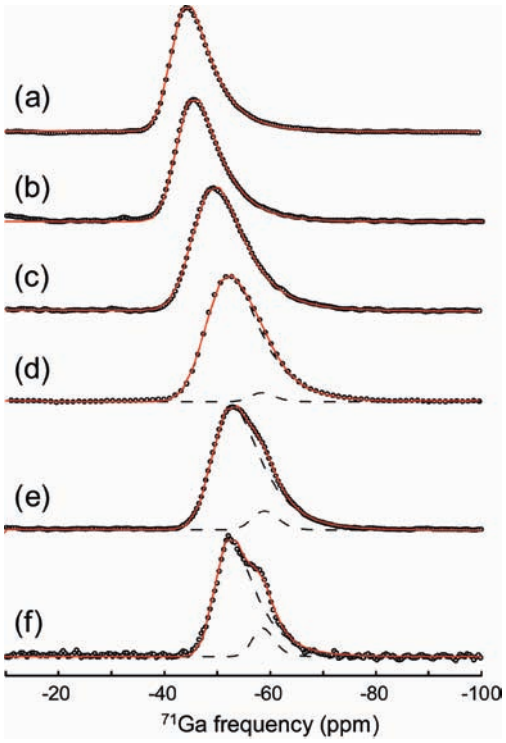

Figure 7. Experimental (black dots) and reconstructed (red lines) ^{71}Ga central transition MAS NMR spectra (B_0 = 17.6 T, MAS 14 kHz) of the $Ca_{10.5-1.5x}Ga_x(PO_4)_7$ compounds with: (a) x = 0.19 (initial Ga/Ca = 0.019), (b) x = 0.22 (initial Ga/Ca = 0.021), (c) x = 0.52 (initial Ga/Ca = 0.052), (d) x = 0.67 (initial Ga/Ca = 0.070), (e) x = 0.73 (initial Ga/Ca = 0.092), and (f) x = 0.82 (initial Ga/Ca = 0.11).

As shown in Figure 6, the 2D ^{31}P homonuclear DQ−SQ correlation spectra recorded for the $Ca_{10.5-1.5x}Ga_x(PO_4)_7$ compounds exhibited enhanced spectral resolution with respect to conventional 1D MAS spectra, giving evidence of the presence of five distinct resonances in the −1.5/−3.0 ppm range. Good fits of both the experimental ^{31}P 2D correlation and 1D quantitative MAS spectra were obtained using the 16 resonances previously observed in pure β-TCP, in addition to these 5 upfield-shifted supplementary lines, the relative intensities of which gradually increased with the Ga content in the structure. Since these resonances strongly overlapped, their positions and linewidths were constrained to vary ±0.1 and ±0.15 ppm, respectively. Although the strong overlap between the ^{31}P resonance prohibited an accurate quantification of the various P sites as a function of the Ga content, the intensity ratio between the two sets of resonance determined following this protocol was found to be in good agreement with the x value in the $Ca_{10.5-1.5x}Ga_x(PO_4)_7$ structure.

To probe the gallium local environment in the $Ca_{10.5-1.5x}Ga_x(PO_4)_7$ structure, ^{71}Ga solid-state MAS NMR experiments were performed at high-magnetic field (17.6 T). As shown in Figure 7, the experimental ^{71}Ga (I = 3/2) MAS NMR spectra of the $Ca_{10.5-1.5x}Ga_x(PO_4)_7$ compounds exhibited asymmetric line shapes which are characteristic of a distribution of the quadrupolar interaction. To account for this distribution of the quadrupolar interaction, the ^{71}Ga MAS NMR line shapes were reconstructed according to the Gaussian isotropic model (GIM) (d = 5, case of the Czjzek distribution)[64] in which the distribution of the electric field gradient is assumed to correspond to a statistical disorder.[65,66] Using this model, good fits of the experimental spectra were obtained, from which the mean ^{71}Ga isotropic chemical shift, the isotropic chemical shift distribution, and the mean quadrupolar coupling product P_Q were determined (ESI, Table 1). The obtained ^{71}Ga isotropic chemical shifts, which range between −39 and −57 ppm, are characteristic of GaO_6 sites,[67,68] in agreement with the proposed $Ca_{10.5-1.5x}Ga_x(PO_4)_7$ structure. It should be noticed that, while the experimental spectra of samples with x < 0.6 are nicely reconstructed with a single contribution, an additional resonance of weaker intensity must be taken into account to obtain good fits of the spectra recorded for the compounds with a x Ga content larger than 0.6. The relative intensity of this additional resonance (with a smaller quadrupolar product and shifted upfield relative to the main peak) increased from 3 to 11% with increasing x from 0.67 to 0.82. Both its quadrupolar product and ^{71}Ga isotropic chemical shift likely indicate the appearance in the structure of more symmetric GaO_6 environments with a larger number of Ga atoms in the remote coordination sphere.

As previously mentioned, for initial Ga/Ca molar ratios higher than 0.075, increasing amounts of side products were detected in the obtained $Ca_{10.5-1.5x}Ga_x(PO_4)_7$ phase, a significant part of which consisting of an amorphous component. The latter was unambiguously identified as poorly crystalline gallium phosphate ($GaPO_4$) from its characteristic ^{31}P and ^{71}Ga isotropic chemical shifts at −9.0 and 117 ppm, respectively (data not shown). This gives evidence that the M5 site cannot be fully substituted by gallium, resulting in a side reaction between gallium and phosphate precursors when the gallium insertion limit ($x \approx 0.8$) is reached.

Finally, it is worth noting that the compressive strength of gallium-doped β-TCP ceramics increases linearly with the Ga content (see Supporting Information). For the higher Ga-substitution rates (21.5 MPa, x = 0.73), the compressive strength was 2.6 times higher than that measured for pure β-TCP (8.3 MPa, x = 0). This is an interesting feature since improved mechanical properties results in better handling of macroporous ceramics for surgeons.

4. CONCLUSION

We have shown that adding a source of gallium during the synthesis of β-TCP, either by direct solid-phase synthesis or calcination of calcium deficient apatite precursors, yielded Ga-doped ceramics as a result of gallium insertion in the β-TCP structure (i.e., $Ca_{10.5-1.5x}Ga_x(PO_4)_7$). This occurs by substitution of one of the five calcium sites in the β-TCP network (M5 site) with a random Ca/Ga distribution, while occupation of another Ca site (M4 site) decreases in inverse proportion to the gallium content. A decrease of the unit cell volume is observed with increasing gallium content, together with improved mechanical properties. However, to avoid the formation of undesired side products (mainly gallium phosphate) in the resulting $Ca_{10.5-1.5x}Ga_x(PO_4)_7$ ceramics, the Ga/Ca ratio used in the synthesis has to be less than 0.075.

Given our recent studies showing that Ga^{3+} ions in solution exhibited a dose-dependent antiresorptive effect[31] and considering that calcium phosphate-based implants are widely used in orthopedics and dentistry for bone tissue engineering, the gallium-doped β-TCP ceramics reported in this study could offer a potential route to induce local Ga^{3+}-mediated bone resorption inhibition in osteoporotic sites. This local drug delivery

approach could offer a convenient strategy to minimize adverse effects reported for long-term systemic gallium treatments and more interestingly increase the gallium bioavailability.

The investigation of the in vivo behavior of these gallium-doped phases is currently underway using an osteoporotic animal model,[11] in addition to the development of suitable protocols for the incorporation of gallium ions in the formulation of injectable calcium phosphate cements, implantable by minimally invasive surgical routes.

■ ASSOCIATED CONTENT

Supporting Information. Experimental details about atomic absorption analyses, transmission electron microscopy, infrared spectroscopy experiments, and mechanical properties measurements. Experimental data obtained from infrared spectroscopy experiments and mechanical properties measurements. This material is available free of charge via the Internet at http://pubs.acs.org.

■ AUTHOR INFORMATION

Corresponding Author

*E-mail (F.F.): fayon@cnrs-orleans.fr; Telephone: +33 2-38-25-55-25. E-mail (B.B.): bruno.bujoli@univ-nantes.fr; Telephone: +33 2-51-12-54-21.

■ ACKNOWLEDGMENT

This work was partially supported by ANR (BiotecS 2008 program grant ANR-08-BIOT-008-02) and the Graftys company. Financial support from the TGIR RMN THC FR3050 for conducting the research is gratefully acknowledged.

■ DEDICATION

This paper is dedicated to Dr. Christian Bruneau on the occasion of his 60th Birthday.

■ REFERENCES

(1) Cavagna, R.; Daculsi, G.; Bouler, J.-M. *J. Long-Term Eff. Med. Implants* **1999**, *9* (4), 403.
(2) Dorozhkin, S.; Epple, M. *Angew. Chem., Int. Ed.* **2002**, *41*, 3130.
(3) Dorozhkin, S. V. *J. Mater. Sci.* **2007**, *42* (4), 1061.
(4) Gouin, F.; Delecrin, J.; Passuti, N.; Touchais, S.; Poirier, P.; Bainvel, J. V. *Rev. Chir. Orthop. Reparatrice Appar. Mot.* **1995**, *81* (1), 59.
(5) Passuti, N.; Daculsi, G. *Presse Med.* **1989**, *18* (1), 28.
(6) Passuti, N.; Daculsi, G.; Rogez, J. M.; Martin, S.; Bainvel, J. V. *Clin. Orthop.* **1989**, *46* (248), 169.
(7) Ransford, A. O.; Morley, T.; Edgar, M. A.; Webb, P.; Passuti, N.; Chopin, D.; Morin, C.; Michel, F.; Garin, C.; Pries, D. *J. Bone Jt. Surg., Br. Vol.* **1998**, *80* (1), 13.
(8) Vallet-Regi, M.; Gonzalez-Calbet, J. M. *Prog. Solid State Chem.* **2004**, *32* (1−2), 1.
(9) Wang, L. J.; Nancollas, G. H. *Chem. Rev.* **2008**, *108* (11), 4628.
(10) Yoshinari, M.; Oda, Y.; Inoue, T.; Matsuzaka, K.; Shimono, M. *Biomaterials* **2002**, *23*, 2879.
(11) Verron, E.; Gauthier, O.; Janvier, P.; Pilet, P.; Lesoeur, J.; Bujoli, B.; Guicheux, J.; Bouler, J.-M. *Biomaterials* **2010**, *31* (30), 7776.
(12) Roussiere, H.; Montavon, G.; Laïb, S.; Janvier, P.; Alonso, B.; Fayon, F.; Petit, M.; Massiot, D.; Bouler, J. M.; Bujoli, B. *J. Mater. Chem.* **2005**, *15* (35−36), 3869.
(13) Peter, B.; Pioletti, D. P.; Laib, S.; Bujoli, B.; Pilet, P.; Janvier, P.; Guicheux, J.; Zambelli, P. Y.; Bouler, J. M.; Gauthier, O. *Bone* **2005**, *36* (1), 52.
(14) Peter, B.; Gauthier, O.; Laib, S.; Bujoli, B.; Guicheux, J.; Janvier, P.; van Lenthe, G. H.; Muller, R.; Zambelli, P. Y.; Bouler, J. M.; Pioletti, D. P. *J. Biomed. Mater. Res. A* **2006**, *76A* (1), 133.
(15) Panzavolta, S.; Torricelli, P.; Bracci, B.; Fini, M.; Bigi, A. *J. Inorg. Biochem.* **2009**, *103* (1), 101.
(16) Nancollas, G. H.; Tang, R.; Phipps, R. J.; Henneman, Z.; Gulde, S.; Wu, W.; Mangood, A.; Russell, R. G. G.; Ebetino, F. H. *Bone* **2006**, *38* (5), 617.
(17) Josse, S.; Faucheux, C.; Soueidan, A.; Grimandi, G.; Massiot, D.; Alonso, B.; Janvier, P.; Laib, S.; Pilet, P.; Gauthier, O.; Daculsi, G.; Guicheux, J.; Bujoli, B.; Bouler, J.-M. *Biomaterials* **2005**, *26* (14), 2073.
(18) Josse, S.; Faucheux, C.; Soueidan, A.; Grimandi, G.; Massiot, D.; Alonso, B.; Janvier, P.; Laib, S.; Gauthier, O.; Daculsi, G.; Guicheux, J.; Bujoli, B.; Bouler, J. M. *Adv. Mater.* **2004**, *16* (16), 1423.
(19) Gao, Y.; Zou, S.; Liu, X.; Bao, C.; Hu, J. *Biomaterials* **2009**, *30* (9), 1790.
(20) Bobyn, J. D.; McKenzie, K.; Karabasz, D.; Krygier, J. J.; Tanzer, M. *J. Bone Jt. Surg., Am. Vol.* **2009**, *91A*, 23.
(21) Boanini, E.; Torricelli, P.; Gazzano, M.; Giardino, R.; Bigi, A. *Biomaterials* **2008**, *29* (7), 790.
(22) Faucheux, C.; Verron, E.; Soueidan, A.; Josse, S.; Arshad, M. D.; Janvier, P.; Pilet, P.; Bouler, J. M.; Bujoli, B.; Guicheux, J. *J. Biomed. Mater. Res., Part A* **2009**, *89A* (1), 46.
(23) Verron, E.; Khairoun, I.; Guicheux, J.; Bouler, J.-M. *Drug Discovery Today* **2010**, *15*, 547.
(24) Schnitzler, V.; Fayon, F.; Despas, C.; Khairoun, I.; Mellier, C.; Rouillon, T.; Massiot, D.; Walcarius, A.; Janvier, P.; Gauthier, O.; Montavon, G.; Bouler, J.-M.; Bujoli, B. *Acta Biomater.* **2011**, *7*, 759.
(25) Gallagher, A. M.; Rietbrock, S.; Olson, M.; van Staa, T. P. *J. Bone Miner. Res.* **2008**, *23* (10), 1569.
(26) Warrell, R. P.; Isaacs, M.; Coonley, C. J.; Alcock, N. W.; Bockman, R. S. *Cancer Treat. Rep.* **1985**, *69* (6), 653.
(27) Warrell, R. P.; Bockman, R. S.; Coonley, C. J.; Isaacs, M.; Staszewski, H. *J. Clin. Invest.* **1984**, *73* (5), 1487.
(28) Bernstein, L. R. *Pharmacol. Rev.* **1998**, *50* (4), 665.
(29) Bockman, R. S.; Wilhelm, F.; Siris, E.; Singer, F.; Chausmer, A.; Bitton, R.; Kotler, J.; Bosco, B. J.; Eyre, D. R.; Levenson, D. *J. Clin. Endocrinol. Metab.* **1995**, *80* (2), 595.
(30) Bockman, R. S.; Bosco, B. *Semin. Arthritis Rheum.* **1994**, *23* (4), 268.
(31) Verron, E.; Masson, M.; Khoshniat, S.; Duplomb, L.; Wittrant, Y.; Baud'huin, M.; Badran, Z.; Bujoli, B.; Janvier, P.; Scimeca, J.-C.; Bouler, J.-M.; Guicheux, J. *Br. J. Pharmacol.* **2010**, *159*, 1681.
(32) Nelson, B.; Hayes, R.; Lowell Edwards, C.; Kniseley, R.; Andrews, G. *J. Nucl. Med.* **1972**, *13* (1), 92.
(33) Dudley, H.; Maddox, G. *J.Pharmacol. Exp. Ther.* **1949**, *96*, 224.
(34) Donnelly, R.; Boskey, A. *Calcif. Tissue Int.* **1989**, *44* (2), 138.
(35) Blumenthal, N. C.; Cosma, V. *Bull. Hosp. Joint Dis. Orthop. Inst.* **1989**, *49* (2), 192.
(36) Melnikov, P.; Teixeira, A. R.; Malzac, A.; Coelho, M. D. *Mater. Chem. Phys.* **2009**, *117* (1), 86.
(37) Korbas, M.; Rokita, E.; Meyer-Klaucke, W.; Ryczek, J. *J. Biol. Inorg. Chem.* **2004**, *9* (1), 67.
(38) Schroeder, L. W.; Dickens, B.; Brown, W. E. *J. Solid State Chem.* **1977**, *22* (3), 253.
(39) Obadia, L.; Deniard, P.; Alonso, B.; Rouillon, T.; Jobic, S.; Guicheux, J.; Julien, M.; Massiot, D.; Bujoli, B.; Bouler, J. M. *Chem. Mater.* **2006**, *18* (6), 1425.
(40) Legrouri, A.; Romdhane, S. S.; Lenzi, J.; Lenzi, M.; Bonel, G. *J. Mater. Sci.* **1996**, *31* (9), 2469.
(41) Kannan, S.; Goetz-Neunhoeffer, F.; Neubauer, J.; Ferreira, J. M. F. *J. Am. Ceram. Soc.* **2009**, *92* (7), 1592.
(42) Enderle, R.; Gotz-Neunhoeffer, F.; Gobbels, M.; Muller, F. A.; Greil, P. *Biomaterials* **2005**, *26* (17), 3379.
(43) Bigi, A.; Foresti, E.; Gandolfi, M.; Gazzano, M.; Roveri, N. *J. Inorg. Biochem.* **1997**, *66* (4), 259.
(44) Benarafa, A.; Kacimi, M.; Coudurier, G.; Ziyad, M. *Appl. Catal., A* **2000**, *196* (1), 25.

(45) Belik, A. A.; Izumi, F.; Stefanovich, S. Y.; Malakho, A. P.; Lazoryak, B. I.; Leonidov, I. A.; Leonidova, O. N.; Davydov, S. A. *Chem. Mater.* **2002**, *14* (7), 3197.
(46) Morozov, V. A.; Belik, A. A.; Stefanovich, S. Y.; Grebenev, V. V.; Lebedev, O. I.; Van Tendeloo, G.; Lazoryak, B. I. *J. Solid State Chem.* **2002**, *165* (2), 278.
(47) Lazoryak, B. I.; Morozov, V. A.; Belik, A. A.; Khasanov, S. S.; Shekhtman, V. S. *J. Solid State Chem.* **1996**, *122* (1), 15.
(48) Petricek, V.; Dusek, M.; Palatinus, L., Jana2006. *The crystallographic computing system.* Institute of Physics, Academy of Sciences of the Czech Republic: Prague (Czech Republic), 2006.
(49) Cheary, R. W.; Coelho, A. A. *J. Appl. Crystallogr.* **1998**, *31*, 862.
(50) Orlhac, X.; Fillet, C.; Deniard, P.; Dulac, A. M.; Brec, R. *J. Appl. Crystallogr.* **2000**, *34*, 114.
(51) Hohwy, M.; Jakobsen, H. J.; Eden, M.; Levitt, M. H.; Nielsen, N. C. *J. Chem. Phys.* **1998**, *108* (7), 2686.
(52) States, D. J.; Haberkorn, R. A.; Ruben, D. J. *J. Magn. Reson.* **1982**, *48* (2), 286.
(53) Trebosc, J.; Hu, B.; Amoureux, J. P.; Gan, Z. *J. Magn. Reson.* **2007**, *186* (2), 220.
(54) Gan, Z. H.; Amoureux, J. P.; Trebosc, J. *Chem. Phys. Lett.* **2007**, *435* (1−3), 163.
(55) Massiot, D.; Fayon, F.; Capron, M.; King, I.; Le Calve, S.; Alonso, B.; Durand, J. O.; Bujoli, B.; Gan, Z. H.; Hoatson, G. *Magn. Reson. Chem.* **2002**, *40* (1), 70.
(56) Dickens, B.; Lw, Schroede.; Brown, W. E. *J. Solid State Chem.* **1974**, *10* (3), 232.
(57) Yashima, M.; Sakai, A.; Kamiyama, T.; Hoshikawa, A. *J. Solid State Chem.* **2003**, *175* (2), 272.
(58) King, I. J.; Fayon, F.; Massiot, D.; Harris, R. K.; Evans, J. S. O. *Chem. Commun.* **2001**, No. 18, 1766.
(59) Perdew, J. P.; Burke, K.; Ernzerhof, M. *Phys. Rev. Lett.* **1996**, *77* (18), 3865.
(60) Pickard, C. J.; Mauri, F. *Phys. Rev. B* **2001**, *63*, 24.
(61) Segall, M. D.; Lindan, P. J. D.; Probert, M. J.; Pickard, C. J.; Hasnip, P. J.; Clark, S. J.; Payne, M. C. *J. Physics-Condensed Matter* **2002**, *14* (11), 2717.
(62) Clark, S. J.; Segall, M. D.; Pickard, C. J.; Hasnip, P. J.; Probert, M. J.; Refson, K.; Payne, M. C. *Z. Kristallogr.* **2005**, *220* (5−6), 567.
(63) Jay, E. E.; Michie, E. M.; Parfitt, D.; Rushton, M. J. D.; Fong, S. K.; Mallinson, P. M.; Metcalfe, B. L.; Grimes, R. W. *J. Solid State Chem.* **2010**, *183* (10), 2261.
(64) Czjzek, G.; Fink, J.; Gotz, F.; Schmidt, H.; Coey, J. M. D.; Rebouillat, J. P.; Lienard, A. *Phys. Rev. B* **1981**, *23* (6), 2513.
(65) Le Caer, G.; Bureau, B.; Massiot, D. *J. Phys.: Condens. Matter* **2010**, *22* (6), 065402.
(66) Le Caer, G.; Brand, R. A. *J. Phys.: Condens. Matter* **1998**, *10* (47), 10715.
(67) Montouillout, V.; Morais, C. M.; Douy, A.; Fayon, F.; Massiot, D. *Magn. Reson. Chem.* **2006**, *44* (8), 770.
(68) Massiot, D.; Vosegaard, T.; Magneron, N.; Trumeau, D.; Montouillout, V.; Berthet, P.; Loiseau, T.; Bujoli, B. *Solid State Nucl. Magn. Reson.* **1999**, *15* (3), 159.